Available online at www.sciencedirect.com
ScienceDirect
Icarus 184 (2006) 338–343
ICARUS
www.elsevier.com/locate/icarus

Minor element evidence that Asteroid 433 Eros is a space-weathered ordinary chondrite parent body

C.N. Foley [a], L.R. Nittler [a,*], T.J. McCoy [b], L.F. Lim [c], M.R.M. Brown [b,d], R.D. Starr [e], J.I. Trombka [c]

[a] *Department of Terrestrial Magnetism, Carnegie Institution of Washington, 5241 Broad Branch Road, NW, Washington, DC 20015-1305, USA*
[b] *Department of Mineral Sciences, National Museum of Natural History, Smithsonian Institution, Washington, DC 20560-0119, USA*
[c] *NASA Goddard Spaceflight Center, Bldg. 2, Code 691, Greenbelt, MD 20771, USA*
[d] *Department of Geological Sciences, Arizona State University, Tempe, AZ 85287-1404, USA*
[e] *Department of Physics, The Catholic University of America, Washington, DC 20064, USA*

Received 27 January 2006; revised 11 May 2006

Available online 5 July 2006

Abstract

The NEAR mission to 433 Eros provided detailed data on the geology, mineralogy, and chemistry of this S-class asteroid [McCoy, T.J., Robinson, M.S., Nittler, L.R., Burbine, T.H., 2002. Chem. Erde 62, 89–121; Cheng, A.F., 1997. Space Sci. Rev. 82, 3–29] with a key science goal of understanding the relationship between asteroids and meteorites [Cheng, A.F., 1997. Space Sci. Rev. 82, 3–29; Gaffey, M.J., Burbine, T.H., Piatek, J.L., Reed, K.L., Chaky, D.A., Bell, J.F., Brown, R.H., 1993a. Icarus 106, 573–602]. Previously reported major element data revealed a bulk surface similar to that of ordinary chondrites, with the notable exception of sulfur, which was highly depleted [Trombka, J.I., and 23 colleagues, 2000. Science 289, 2101–2105; Nittler, L.R., and 14 colleagues, 2001. Meteorit. Planet. Sci. 36, 1673–1695]. The origin of this sulfur deficiency, and hence the fundamental nature of the asteroid's surface, has remained controversial. We report a new analysis of NEAR X-ray spectrometer data, indicating that Eros has Cr/Fe, Mn/Fe, and Ni/Fe ratios similar to ordinary chondrite meteorites of type LL or L. Chondritic levels of Cr, Mn, and Ni argue strongly against a partial melting explanation for the sulfur depletion. Instead, our results provide definitive evidence that Eros is a primitive body with composition and mineralogy similar to ordinary chondrites, but with a surface heavily modified by interactions with the solar wind and micrometeorites, processes collectively termed space weathering.

Keywords: Asteroids, composition; Solar radiation; Meteorites; Spectroscopy; Asteroids, surfaces

1. Introduction

It has been hypothesized for some time (Gaffey et al., 1993) that some S-asteroids, the most abundant in the inner asteroid belt, are the source of ordinary chondrites, the most abundant meteorites on Earth. Mineralogical data from the near infrared spectrometer (NIS) and chemical data from the X-ray (XRS) and gamma-ray (GRS) spectrometers on the NEAR spacecraft largely support such a connection, but the XRS data revealed a surprise (Trombka et al., 2000; Nittler et al., 2001). Although the major element ratios Mg/Si, Al/Si, Ca/Si, and Fe/Si, determined by XRS (Nittler et al., 2001), and the Fe/Si, O/Si ratios and the K abundance determined by GRS (Evans et al., 2001) are consistent with an undifferentiated body of approximately ordinary chondrite composition, sulfur was found to be strongly depleted at the surface. The XRS measurement indicated an upper limit for S/Si of 0.05 (Nittler et al., 2001), more than a factor of two lower than the typical value of 0.11 for ordinary chondrites.

Two explanations for the low sulfur abundance have been proposed, with broad implications for the nature and history of Eros (Trombka et al., 2000; Nittler et al., 2001) and for the understanding of remote sensing data from other asteroids. First, Eros might have a bulk ordinary chondrite composition, but impact and/or radiation processes (space weathering) removed the volatile sulfur from the surface layers. Such processes are often invoked to explain differences in reflectance spectra of

* Corresponding author. Fax: +1 202 478 8821.
E-mail address: lrn@dtm.ciw.edu (L.R. Nittler).

0019-1035/$ – see front matter
doi:10.1016/j.icarus.2006.05.011

S-asteroids and ordinary chondrites (Chapman, 2004; Hapke, 2001). Second, Eros might have undergone a limited amount of partial melting, with loss of a sulfur-rich melt, perhaps into the asteroid's interior. In this case, Eros would have had a different thermal history than the parent bodies of known ordinary chondrite meteorites. The first explanation, that Eros is a space-weathered, undifferentiated body with ordinary chondrite-like composition, has been favored, but significant controversy over the nature of Eros' surface and history persists (Cheng, 2002; McFadden et al., 2005). We report here the measurement of minor elements particularly sensitive to partial melting: Cr, Mn, and Ni. Partial melting leads to non-chondritic abundances of these elements while space weathering does not, which makes them particularly useful to resolve this debate.

2. Analyses of NEAR XRS data

The NEAR XRS detected 1–10 keV X-rays from the top tens of microns of the surface of Eros and has been described in detail elsewhere (Nittler et al., 2001; Starr et al., 2000; Trombka et al., 1997). Measured X-ray spectra include fluorescent emission induced by solar X-rays as well as coherently and incoherently scattered solar X-rays. Because of their low abundances, detection of fluorescent X-rays from Cr (Kα = 5.4 keV), Mn (Kα = 5.9 keV), and Ni (Kα = 7.5 keV) was only possible during solar flares, when the solar X-ray flux increases by orders of magnitude, especially at the higher energies needed to induce emission from these elements. We have analyzed data for two flares containing the highest signal in the >5 keV region of the spectra, from May 4, 2000 and December 27, 2000. To increase the signal-to-noise ratio, spectra for each flare collected by the three separate (unfiltered, Mg-filtered and Al-filtered) asteroid-facing detectors were co-added following appropriate correction for slightly different energy-channel calibrations (Fig. 1). Following background subtraction, spectral fitting was used to derive X-ray fluorescence intensities for Cr, Mn, Fe, and Ni and these were converted to elemental ratios using theoretical calibration curves appropriate to the observed solar incident spectra during the flares (Lim, 2005; Nittler et al., 2001).

In addition to the cosmic ray background, theoretical (Nittler et al., 2001) coherently-scattered solar X-ray spectra were also subtracted from the Eros spectra. This latter background was modeled using an LL chondrite bulk composition and the appropriate incident solar spectra for each flare (Fig. 1) and scaled to the observed spectra before subtraction. Differences in model scatter spectra among ordinary chondrite subclasses are small and our choice of an LL chondrite does not introduce significant systematic uncertainty. Gaussian areas were then computed by spectral fitting (Fig. 1) using a commercial program (Peak-fit, Systat Software, Inc.) and converted to photon ratios by accounting for the known detector efficiencies (Starr et al., 2000) as a function of energy. Photon ratios were converted to element ratios using calibration curves derived from theoretical X-ray fluorescence models of twenty meteorites with varying compositions (Nittler et al., 2001, 2004) and incident solar spectra derived from NEAR solar monitor data for the appropriate flares (Lim et al., 2005; Lim, 2005). The validity of the technique was tested using synthetic spectra generated with similar counting statistics to the NEAR spectra and varying Mn, Cr, and Ni abundances.

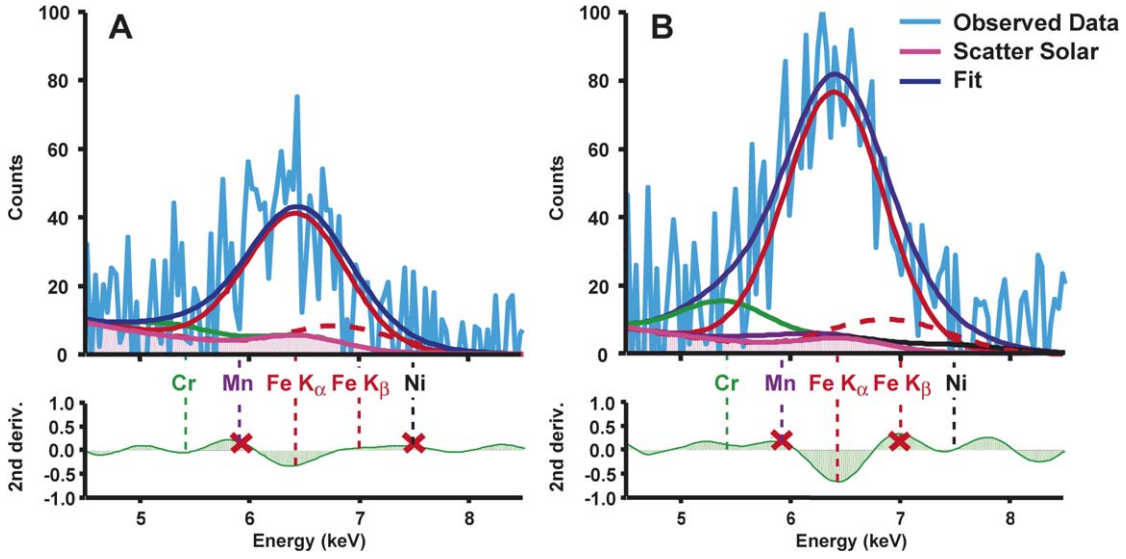

Fig. 1. Fe region of XRS spectrum from December 27, 2000 solar flare. (A) The signal from only the unfiltered detector and (B) the summed signal from the unfiltered, Mg-filtered, and Al-filtered detectors. The light blue lines show the NEAR XRS data (with cosmic-ray induced detector background subtracted), the shaded pink areas are the modeled coherently scattered solar background and the dark blue smooth lines are the total fits to the data. Scattered background is scaled to match the observed spectrum in regions where no significant fluorescence intensity should be present. Minima in the second derivatives of the summed Gaussian fits, shown at the base of each spectrum, indicate detected peaks. Individual Gaussian fits for the detected peaks are shown (green, Cr; purple, Mn; red solid line, Fe Kα; red dashed line, Fe Kβ; black, Ni). The Fe Kβ peaks for both (A)–(B) are below the detection limit and are not measured, but are set from the theoretical Fe Kα/Kβ ratio. The significantly larger signal from the summed spectrum of (B) enables measurement of Ni and measurement of Cr with a higher signal/noise ratio; thus summed spectra were used to determine abundances from both flares. Although Mn is shown in (B), its detection is not statistically significant.

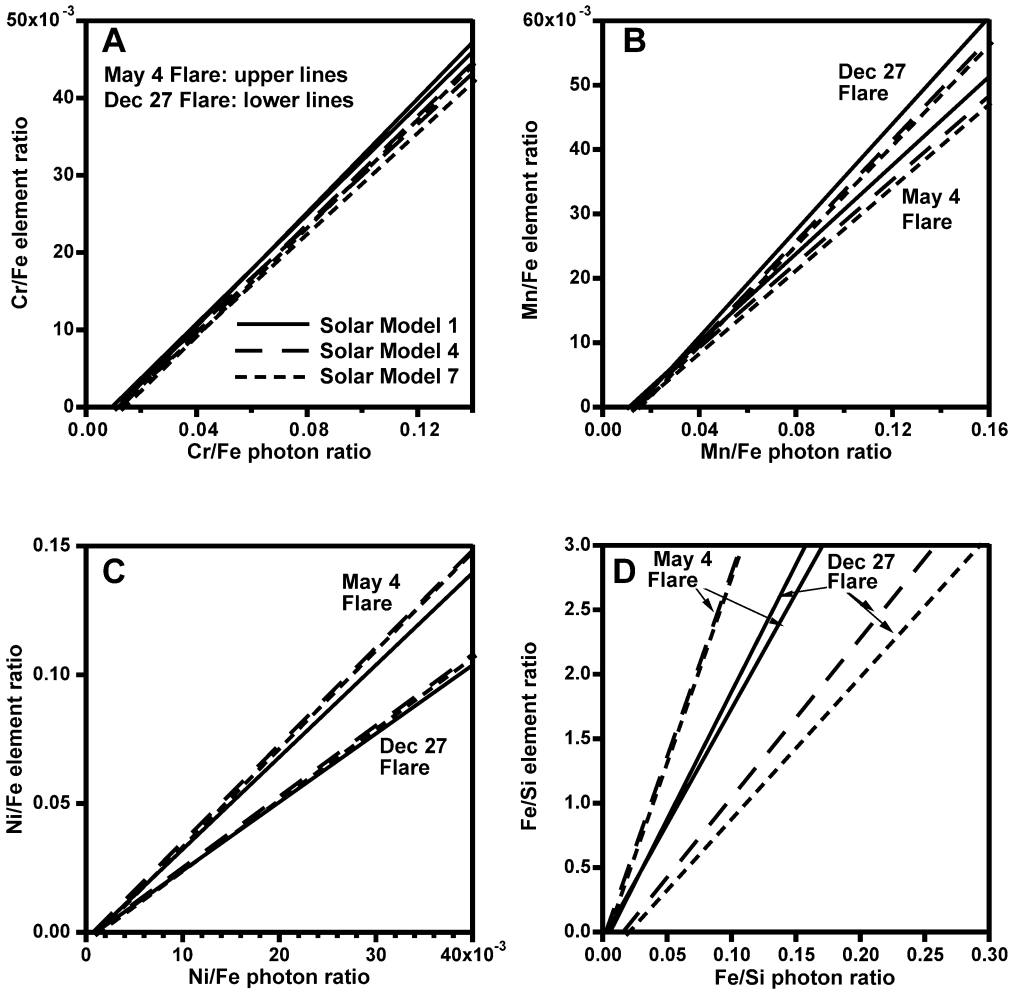

Fig. 2. Calibration curves used to determine elemental abundance ratios from derived photon ratios for Cr/Fe, Mn/Fe, Ni/Fe, and Fe/Si. These curves are dependent upon the measured solar spectra during the flares, XRF models from Nittler et al. (2001), and solar models 1, 4, and 7 [the most accurate models from the seven described by Lim (2005)]. Of these parameters, only uncertainties in the solar models yield significantly different results. The resulting calibration curves for the solar models 1, 4, and 7 are shown as solid, long-dashed and short-dashed, respectively. Only for element pairs such as Fe and Si, which are generated by different energy regions of the solar spectrum, do the differences in the solar models generate potentially large systematic errors. Cr/Fe, Mn/Fe, and Ni/Fe are not subject to large uncertainties due to solar model variations, as evident by the similarity between the calibration curves for all three models. The relatively small differences between these curves are taken into account in calculating the errors on the derived element ratios (Table 1), however.

Model solar spectra are based on improved modeling of the NEAR solar monitor and improved solar physics (Lim et al., 2005; Lim, 2005), compared to spectra previously used by Nittler et al. (2001). Although remaining uncertainties mean that a range of models can explain the observed solar spectra equally well and these models lead to a range of calibration curves, the >2.5 keV region of the spectra is much less sensitive to variations in the solar models than is the lower-energy portion. We thus ratioed the minor elements to Fe, rather than the Si normalization previously used for major elements (Nittler et al., 2001), to minimize remaining systematic uncertainties from solar modeling. We report averages for each flare of results derived from three solar models that reproduce the observed solar spectra during the analyzed flares.

Calibration curves for Cr/Fe, Mn/Fe, and Ni/Fe ratios are shown in Fig. 2. These curves indicate the predicted X-ray fluorescence ratio for the specified elements as a function of the composition ratio (taken from a wide range of bulk meteorite measurements: Nittler et al., 2001, 2004) for a given input solar spectrum and viewing geometry appropriate to the specific flare. The three curves correspond to those from Lim (2005) that best match the NEAR solar monitor spectra for the given flares. Differences in the solar monitor models for these minor elements do not result in significant differences in the computed elemental ratios, because these elements are excited from a relatively limited region of the incident solar X-ray spectrum (near the strong Fe emission around 6 keV). In contrast, the different models have a much larger effect on the relative intensities of elements like silicon and iron, which are generated from more widely spaced regions of the solar spectrum (Fig. 2). Similarly, Fe/Si is more strongly affected by shadowing effects during spectral acquisition at high phase angles (Okada, 2004). Thus, Cr/Fe, Mn/Fe, and Ni/Fe ratios determined by remote-sensing X-ray spectroscopy are less susceptible to systematic errors in solar monitor modeling than is the Fe/Si ratio.

In previous work (Nittler et al., 2001), a "mineral mixing correction" was applied to the XRS element ratios to account for the probability that Eros may not be geochemically homogeneous on a scale of tens of μm (the approximate scale length of the X-ray production and emission), but may have elements concentrated within specific minerals. This correction would increase our inferred Cr/Fe ratios by as much as a factor of two and also strongly affect Ni abundances. While the degree of fine-scale heterogeneity on Eros' surface is not known, it is likely to be comparable to a well-mixed homogeneous powder due to impact processing. X-ray calibration data from the Mars Pathfinder APXS (Foley, 2002) for finely-ground samples (i.e., grains on the order of tens of μm) of the Murchison (CM2), Allende (CV3), and Bruderheim (L6) meteorites indicate no difference within 1σ between the determined major and minor rock-forming element ratios (computed with the X-ray mode) and those determined by standard methods for bulk chemical analyses (e.g., wet chemistry). In fact, modeling of S-asteroid reflectance spectra (Hapke, 2001) suggests regoliths are comprised of grain sizes on the order of 10 μm. Thus, mineral mixing corrections are not applied here to the Eros data. Even without the mineral corrections, the prior (Nittler et al., 2001) conclusion that Eros has an ordinary chondrite-like major-element composition with a depleted S/Si ratio, is still valid.

3. Results

Derived Cr/Fe, Mn/Fe, and Ni/Fe ratios for the two flares are given in Table 1 and plotted in Fig. 3. Fully differentiated meteorites (e.g., eucrites, diogenites) and enstatite chondrites are not shown, because these have been previously ruled out as potential analogs for Eros on the basis of both major-element composition and mineralogy. Cr was clearly identified in both flare spectra and Ni in the December 27 flare. In contrast, the detection limit for Mn was relatively high because the detector resolution was not sufficient to resolve the Mn emission lines from the much stronger Fe signal. Therefore, we can only place an upper limit on the Mn/Fe ratio.

Major element ratios for Eros (Fig. 3) are weighted average values from the five flares reported by Nittler et al. (2001). F1 (two-temperature fit to solar monitor data) was utilized for all flares except for the May 4th and June 15th flares, for which F2 (single temperature fit to solar model data) was used. Errors (2σ) for the major elements were taken as the larger of either the standard error of the mean or the weighted mean error of the individual flare results, with weights based on individual flare counting-statistical errors. Therefore, they do not include uncertainties in the solar X-ray spectral models, which may in particular introduce some systematic errors, especially for Fe/Si (Lim et al., 2005; Lim, 2005).

The minor elements Cr, Mn, and Ni were measured using only the spectra from the two flares (from May 4 and December 27, 2000) which had the largest signal/noise ratios for the iron-region of the X-ray spectra. The 2σ errors given in Table 1 are based on propagation of errors from the spectral fitting (mainly statistical) and systematic errors due to different solar models. The latter are estimated from the range of calibration curves derived for a given flare, as described previously.

4. Interpretations and conclusions

Our derived Cr/Fe and Ni/Fe ratios, the upper limit on the Mn/Fe ratio, and the plotted major element ratios, are clearly consistent with those of ordinary chondrites, particularly the low iron (L and LL) ordinary chondrites (Fig. 3). Note that the Fe/Si ratio is much more susceptible than is Cr/Fe to systematic uncertainties due to errors in solar modeling (Lim et al., 2005; Lim, 2005) and shadowing effects (Okada, 2004). Thus, the Cr/Fe ratio is a more robust indicator of the nature of Eros' surface than the Fe/Si ratio. Although individual ratios overlap in some cases with meteorites other than ordinary chondrites, L and LL chondrites are the only classes that consistently overlap with the Eros results for all derived ratios (except for S/Si). This agrees qualitatively with the mineral chemistry derived from near infrared spectra (Izenberg et al., 2003) and the Fe/Si ratio (0.8 ± 0.3) determined by the NEAR GRS (Evans et al., 2001). However, regolith processes occurring within "ponded" materials (Robinson et al., 2001) at the GRS measurement site may well lead to a different surface Fe abundance there (Evans et al., 2001; McCoy et al., 2001), compared to that of the bulk asteroid's surface and the XRS and GRS results thus would not necessarily be expected to match. In any case, the new minor element ratios rule out both carbonaceous chondrites and known classes of primitive achondrites (partially melted meteorites) as analogs to Eros and provide strong constraints on the origin of the observed sulfur depletion.

Partial melting and space weathering have been suggested as possible explanations for the sulfur deficiency on Eros. Limited partial melting affecting the sulfur abundance also might

Table 1
Minor element composition results for asteroid Eros

Photon ratio	May 4, 2000	December 27, 2000	
Cr/Fe	0.07 ± 0.02	0.09 ± 0.04	
Mn/Fe	0.03 ± 0.04	0.02 ± 0.04	
Ni/Fe	0.03 ± 0.03	0.04 ± 0.02	
Element ratio			Final estimated value (2 flares)
Cr/Fe	0.020 ± 0.007	0.028 ± 0.012	0.022 ± 0.006
Mn/Fe	0.0071 ± 0.014	0.0022 ± 0.016	0.005 ± 0.011; $\leqslant 0.017$
Ni/Fe	–	0.11 ± 0.05	0.11 ± 0.05

Note. Ratios are $\pm 2\sigma$ based on propagation of errors from the spectral fitting (mainly statistical) and systematic errors due to different solar models.

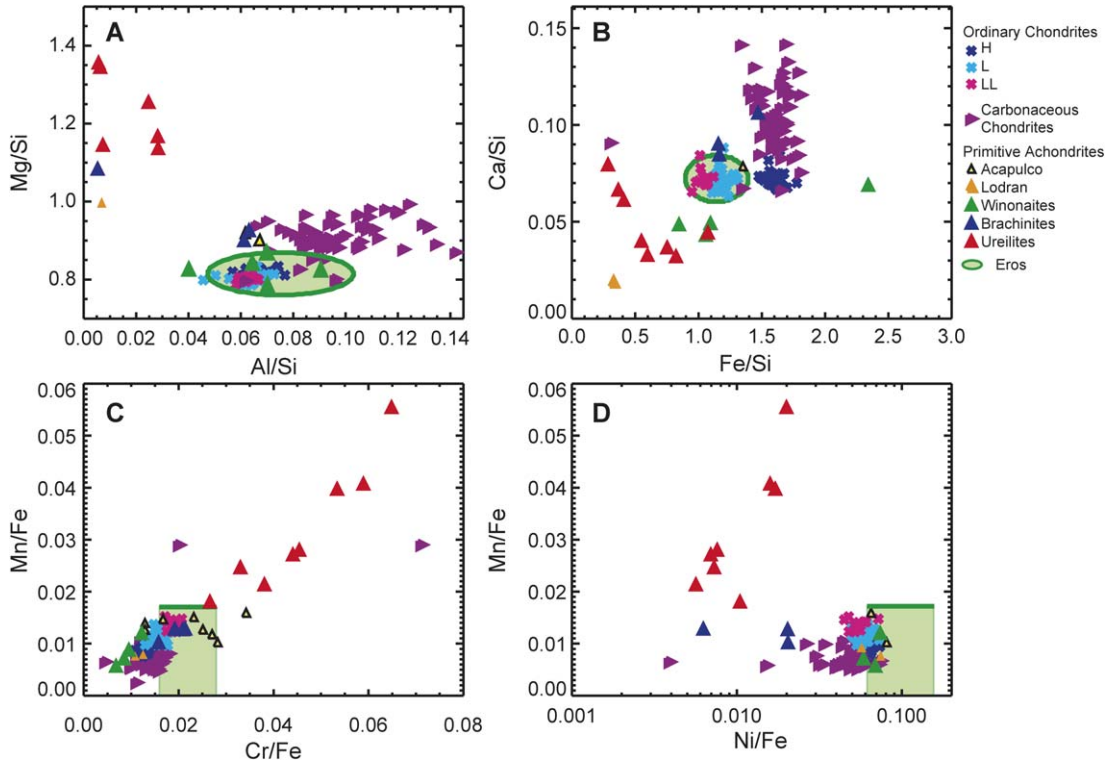

Fig. 3. Weight ratios of (A) Mg/Si versus Al/Si, (B) Ca/Si versus Fe/Si, (C) Mn/Fe versus Cr/Fe, and (D) Mn/Fe versus Ni/Fe at the surface of Eros (2σ errors and/or 3σ upper limits) are compared to a number of meteorites (Nittler et al., 2004). The Cr/Fe, Mn/Fe, and Ni/Fe ratios for Eros, green shaded areas, were determined in this study (Table 1). The major element ratios are the average values previously determined for five flares by Nittler et al. (2001) without mineral mixing corrections applied. Recent calculations for additional flares with improved solar models yield consistent major-element results (Lim et al., 2005; Lim, 2005). Plotted meteorite groups include the carbonaceous and ordinary chondrites and several classes of primitive achondrites. Differentiated meteorites and enstatite chondrites, which have been ruled out as Eros analogs by Nittler et al. (2001) are not plotted. Although some individual primitive achondrite meteorites overlie the average Eros values for some ratios, only L and LL chondrites appear consistent with Eros for all plotted ratios.

strongly affect the abundances of minor elements, especially Cr and Ni. The first partial melt of chondritic material is an Fe,Ni–FeS melt with ~85 wt% FeS (Kullerud, 1963). Removal of this melt would cause depletions in sulfur and to a lesser extent Fe and Ni, relative to silicon. Thus, if the sulfur depletion on Eros was due to loss of an Fe,Ni–FeS melt, Fe and Ni depletions could also be expected. Notably, the Ni/Fe ratios for meteorites believed to be residues of significant partial melting (e.g., lodranites and ureilites, described further below) are significantly sub-chondritic. Moreover, there is evidence that chromite (the dominant mineral carrier of Cr in most ordinary chondrites) would be strongly redistributed during early partial melting. In the EET 84302 lodranite, we have observed melting of chromite, metal and sulfide at mutual junctions and a chromite-rich lithology supportive of Cr entering the early partial melt. Mineral mapping of the primitive achondrites Acapulco and Lodran suggests that the residual Lodran contains half as much chromite (0.7 vol%) as does the broadly chondritic Acapulco (1.6 vol%) from which it may be derived. Calculations for removal of individual minerals indicate that chromite removal would dramatically lower Cr abundances. This is consistent with Lodran exhibiting lower Cr abundances (and Cr/Si and Cr/Fe ratios) than Acapulco (Fukuoka et al., 1978; Palme et al., 1981) (Fig. 3). Since Mn is primarily present in ordinary chondrites in olivine and orthopyroxene, metal–sulfide partial melting would not be expected to significantly affect the Mn bulk abundance. In fact, ureilites have Mn/Fe ratios higher than chondritic, due to loss of Fe-rich melt.

Space-weathering processes (Nittler et al., 2001; Killen, 2003; Kracher and Sears, 2005), such as sputtering by solar wind ions and/or micrometeorite impacts, could effectively deplete the surface sulfur and other volatile species, but not affect the abundances of other rock forming elements. Both processes cause vaporization followed by redeposition or loss of elements leading to darkening and reddening of the visible and near-infrared spectra (Hapke, 2001). In particular, the redeposition of iron in ubiquitous vapor-deposited coatings on regolith particles and inside agglutinates produces the dominant space weathering product which affects reflectance spectra of metallic iron particles smaller than the wavelength (sub-micron) (Hapke, 2001). In contrast some volatile light elements are lost from the space weathered surface, particularly sulfur which is notably lost from the lunar regolith by as much as 30% (Clayton et al., 1974). Alternatively, sulfur mobilization and loss may be due to impact-induced vaporization on the cm-scale causing loss on the dm-scale of OC parent bodies inferred from the presence of troilite veins in the Smyer H-chondrite impact-melt breccia (Rubin, 2002). In contrast, Cr, Mn and Ni should not be strongly affected by space weathering or cm-scale impact vaporization. The mineral carriers of Cr and Mn—chromite and

mafic silicates—are much more resistant than FeS and these elements are much less volatile than S. Metal also could be vaporized relatively quickly by sputtering, though less so than FeS (Kracher and Sears, 2005). However, in this case Fe and Ni would likely be redeposited on the surface and there is in fact evidence for such a process occurring on the Moon (Hapke, 2001). Importantly, this redistribution of Fe (and probably Ni) should not significantly affect the bulk Fe abundance determined by the XRS (which probes the surface chemistry to a depth of tens of microns).

Our observation that Eros has chondritic Cr/Fe and Ni/Fe ratios and a chondritic to sub-chondritic Mn/Fe ratio argues that this asteroid has not undergone partial melting, but has a low surface sulfur abundance due to space weathering processes. Centimeter-scale impact-induced S volatilization may also play a role (Rubin, 2002), but the meteoritic evidence does not suggest that this depletes S to the extent observed on the surface of Eros. Together with additional chemical and mineralogical data from the NEAR XRS, GRS, and NIS instruments, we are converging on a consistent picture that Eros, and perhaps other S-asteroids, closely resembles a space-weathered L or LL ordinary chondrite

Acknowledgments

This work was supported by a NASA Discovery Data Analysis Program grant to L.R.N. We thank Alan Rubin and an anonymous reviewer for constructive comments.

References

Chapman, C.R., 2004. Space weathering of asteroid surfaces. Ann. Rev. Earth Planet. Sci. 32, 539–567.

Clayton, R.N., Mayeda, T.K., Hurd, J.M., 1974. Loss of oxygen, silicon, sulfur, and potassium from the lunar regolith. Proc. Lunar Sci. Conf. 5, 1801–1809.

Cheng, A.F., 2002. Near Earth Asteroid Rendezvous: Mission summary. In: Bottke, W.F., Cellino, A., Paolicchi, P., Binzel, R.P. (Eds.), Asteroids III. Univ. of Arizona Press, Tucson, pp. 351–366.

Evans, L.G., Starr, R.D., Brückner, J., Reedy, R.C., Boynton, W.V., Trombka, J.I., Goldstein, J.O., Masarik, J., Nittler, L.R., McCoy, T.J., 2001. Elemental composition from gamma-ray spectroscopy of the NEAR-Shoemaker landing site on 433 Eros. Meteorit. Planet. Sci. 36, 1639–1660.

Foley, C.N., 2002. Ph.D. dissertation, 252. University of Chicago, Chicago.

Fukuoka, T., Ma, M.S., Wakita, H., Schmitt, R.A., 1978. Lodran: The residue of limited partial melting of matter like a hybrid between H and E chondrites. Lunar Planet. Sci. 9, 356–358.

Gaffey, M.J., Burbine, T.H., Binzel, R.P., 1993. Asteroid spectroscopy—Progress and perspectives. Meteoritics 28, 161–187.

Hapke, B., 2001. Space weathering from Mercury to the asteroid belt. J. Geophys. Res. 106, 10039–10074.

Izenberg, N.R., Murchie, S.L., Bell III, J.F., McFadden, L.A., Wellnitz, D.D., Clark, B.E., Gaffey, M.J., 2003. Spectral properties and geologic processes on Eros from combined NEAR NIS and MSI data sets. Meteorit. Planet. Sci. 38, 1053–1077.

Killen, R.M., 2003. Depletion of sulfur on the surface of asteroids and the Moon. Meteorit. Planet. Sci. 38, 383–388.

Kracher, A., Sears, D.W.G., 2005. Space weathering and the low sulfur abundance of Eros. Icarus 174, 36–45.

Kullerud, G., 1963. The Fe–Ni–S system. Ann. Rep. Geophys. Lab. 67, 4055–4061.

Lim, L.F., Nittler, L.R., Starr, R.D., McClanahan, T.P., 2005. Elemental composition of 433 Eros: New calibration of the NEAR-Shoemaker XRS data. Lunar Planet. Sci. 36. Abstract 2031.

Lim, L.F., 2005. Ph.D. dissertation, 226. Cornell University, Ithaca.

McCoy, T.J., and 16 colleagues, 2001. The composition of 433 Eros: A mineralogical-chemical synthesis. Meteorit. Planet. Sci. 36, 1661–1672.

McFadden, L.A., Goldman, N.J., Gaffey, M.J., Izenberg, N.R., 2005. Evidence for partial melting in reflectance spectra of 433 Eros. Lunar Planet. Sci. 36. Abstract 561.

Nittler, L.R., and 14 colleagues, 2001. X-ray fluorescence measurements of the surface elemental composition of Asteroid 433 Eros. Meteorit. Planet. Sci. 36, 1673–1695.

Nittler, L.R., McCoy, T.J., Clark, P.E., Murphy, M.E., Trombka, J.I., Jarosewich, E., 2004. Bulk element compositions of meteorites: A guide for interpreting remote-sensing geochemical measurements of planets and asteroids. Antarct. Meteorite Res. 17, 233–253.

Okada, T., 2004. Particle size effect in X-ray fluorescence at a large phase angle: Importance on elemental analysis of Asteroid Eros (433). Lunar Planet. Sci. 35. Abstract 1927.

Palme, H., Schultz, L., Spettel, B., Weber, H.W., Wanke, H., Michael-Levy, M.C., Lorin, J.C., 1981. The Acapulco meteorite: Chemistry, mineralogy and irradiation effects. Geochim. Cosmochim. Acta 45, 727–752.

Robinson, M.S., Thomas, P.C., Veverka, J., Murchie, S., Carcich, B., 2001. The nature of ponded deposits on Eros. Nature 413, 396–400.

Rubin, A., 2002. Smyer H-chondrite impact-melt breccia and evidence for sulfur vaporization. Geochim. Cosmochim. Acta 66, 699–711.

Starr, R., and 16 colleagues, 2000. Instrument calibrations and data analysis procedures for the NEAR X-ray spectrometer. Icarus 147, 498–519.

Trombka, J.I., and 12 colleagues, 1997. Compositional mapping with the NEAR X-ray/gamma-ray spectrometer. J. Geophys. Res. 102, 23729–23750.

Trombka, J.I., and 23 colleagues, 2000. The elemental composition of Asteroid 433 Eros: Results of the NEAR-Shoemaker X-ray spectrometer. Science 289, 2101–2105.